Testing strong gravity with gravitational waves and Love numbers

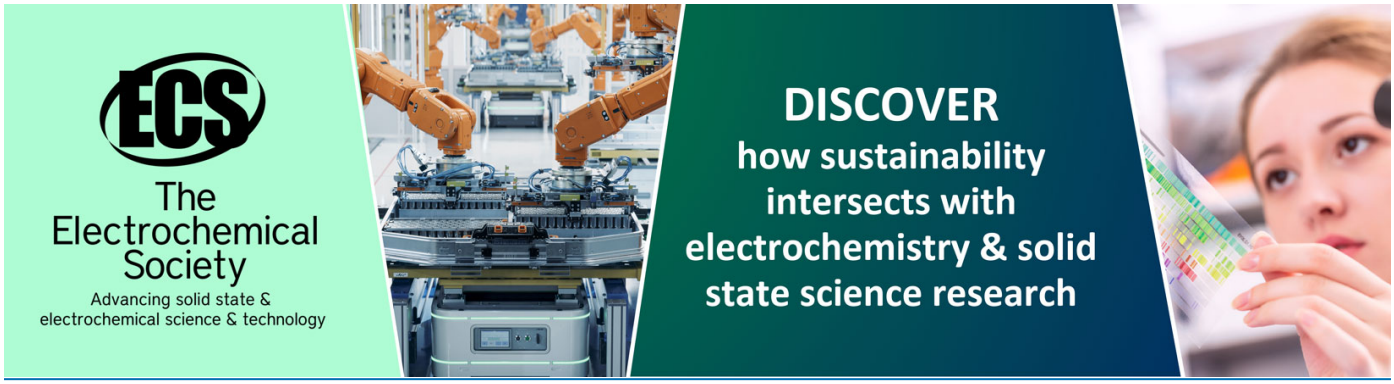

IOP Conf. Series: Journal of Physics: Conf. Series **841** (2017) 012035 doi:10.1088/1742-6596/841/1/012035

Testing strong gravity with gravitational waves and Love numbers

E Franzin,[1] **V Cardoso,**[2,3] **P Pani,**[4,2] **and G Raposo**[2]

[1] Dipartimento di Fisica, Università di Cagliari & INFN, Sezione di Cagliari, Cittadella Universitaria, 09042 Monserrato, Italy
[2] CENTRA, Departamento de Física, Instituto Superior Técnico, Universidade de Lisboa, Av. Rovisco Pais 1, 1049 Lisboa, Portugal
[3] Perimeter Institute for Theoretical Physics, 31 Caroline Street North, Waterloo, Ontario N2L 2Y5, Canada
[4] Dipartimento di Fisica, "Sapienza" Università di Roma & INFN, Sezione di Roma1, p.zza A. Moro 5, 00185, Roma, Italy

E-mail: edgardo.franzin@ca.infn.it

Abstract. The LIGO observation of GW150914 has inaugurated the gravitational-wave astronomy era and the possibility of testing gravity in extreme regimes. While distorted black holes are the most convincing sources of gravitational waves, similar signals might be produced also by other compact objects. In particular, we discuss what the gravitational-wave ringdown could tell us about the nature of the emitting object, and how measurements of the tidal Love numbers could help us in understanding the internal structure of compact dark objects.

1. Introduction

The observations of the GW150914 and GW151226 events by the LIGO/Virgo collaborations have been interpreted as the gravitational waves emitted by a binary stellar-mass black holes merger [1, 2]. These events are characterised by three phases: the inspiral, when the distance between the two companions is large; the merger, when the two objects coalesce; and the ringdown, when the product of the merger relaxes to a stationary equilibrium configuration, with the emission of gravitational waves. The implications on theoretical physics of such mergers have been broadly discussed in [3]. Here, we discuss what gravitational-wave observations can tell us about the nature of the binary companions and the product of the coalescence.

The existence of black holes is supported by various indirect observations in the electromagnetic band, but the detection of GW150914 and GW151226 can be acknowledged as the first direct observation. In addition, the existence of event horizons — the defining property of black holes — might be probed only with gravitational-wave observations, as electromagnetic observations cannot probe the existence of event horizons, but only the existence of a light ring, *i.e.* a boundary within which photons can be trapped in circular orbits [4]. But, is there any evidence for event horizons in the detected signals?

There exist compact objects whose exterior geometry is the same as black holes but without an event horizon: they are called black hole mimickers and they include boson stars [5], wormholes [6], gravastars [7] and superspinars [8]. These objects and black holes are dark and then indistinguishable to electromagnetic instruments. On the other hand, ultra-compact objects

are generically unstable [9], and with the exception of boson stars, there exists no formation mechanism (yet) of black hole mimickers; wormholes and gravastars are rather artificial solutions to Einstein's equations.

In Section 2, we investigate the gravitational radiation emitted by a point particle in radial motion towards a traversable wormhole and we compare it to that of a Schwarzschild black hole. We show that, if the wormhole is compact enough, the distinction in the initial ringdown signal is irrelevant [10].

During the inspiral phase, at large orbital separations (low frequencies) the tidal interaction is negligible. As the orbital separation decreases (higher frequencies), the tidal interaction becomes important. In linear perturbation theory, the relation between the tidal field and the induced moment is constant, and such a constant is known as the tidal Love number.[1] Love numbers encode the information about the deformability of an object in a tidal environment and depend significantly on the object internal structure. Love numbers for black holes in general relativity are identically zero, while this is not the case for black holes in modified theories of gravity and for other exotic compact objects such as boson stars, wormholes and gravastars.

In Section 3, we compute Love numbers for minimal boson stars and gravastars and we discuss their possible detection [12].

We adopt natural units, $c = G = 1$.

2. Ringdown

In general relativity, Quasi-Normal Modes (QNMs) appear in the study of linear perturbations of black hole spacetimes [13, 14]. In most cases, the perturbation equations reduce to a linear second-order differential equation supplemented by boundary conditions at the horizon and at infinity. QNMs are the complex eigenvalues of this equation, with the real part representing the actual frequency of the oscillation and the imaginary part representing the damping.

QNMs were thought to dominate the ringdown waveform, and then the ringdown to be a piece of evidence for black holes. In fact, the black hole QNMs are deeply related to the boundary conditions required at the event horizon, while, for a horizonless object, the boundary conditions change completely, and so the QNM spectrum.

We now show that the ringdown phase should not depend on the presence of a horizon as long as the final object is compact enough to possess a light ring. For a black hole, the ringdown phase is described by the QNMs *by accident*, as the ringdown waves are carried inside the black hole because of the ingoing condition at the horizon. For another horizonless object, its relaxation consists of the light ring ringdown modes (insensitive to the boundary conditions), followed by the proper modes of vibration (read QNMs) of the object itself.

2.1. Traversable Wormholes

We study the gravitational radiation emitted by a point particle that plunges radially in a traversable wormhole and emerges in another universe.

The mimicker is built with two copies of Schwarzschild with the same mass M,

$$\mathrm{d}s^2 = -\left(1-\frac{2M}{r}\right)\mathrm{d}t^2 + \left(1-\frac{2M}{r}\right)^{-1}\mathrm{d}r^2 + r^2\,\mathrm{d}\Omega^2, \tag{1}$$

glued together at the throat $r = r_0 > 2M$. Such a surgery at the throat requires a thin shell of matter with surface density σ and surface pressure p. In general relativity, the matter content satisfies some energy conditions: for a perfect fluid, the null and strong energy conditions put constraints on combinations of σ and p, while the weak energy condition adds that $\sigma \geqslant 0$. In

[1] When the orbital motion approaches a resonance, the relation between the induced quadrupole moment and the tidal field is no longer constant, and the tides become dynamical [11].

order to have a traversable wormhole in general relativity, the weak energy condition must be violated, meaning that σ is negative. The null and strong energy conditions are satisfied when the throat is within the light ring [15].

In the point-particle limit, the Einstein equations reduce to a pair of Zerilli equations [16],

$$\frac{\mathrm{d}^2\psi_\ell(\omega,r)}{\mathrm{d}r_*^2}+\left[\omega^2-V_\ell(r)\right]\psi_\ell(\omega,r)=S_\ell\,, \tag{2}$$

where r_* is the tortoise coordinate and $\ell\geqslant 2$ is the index of the spherical-harmonic expansion. Notice that the source term is different in the two universes.

The QNMs of the wormhole are defined by the eigenvalue problem associated with Eq. (2) when $S_\ell=0$, supplemented by regularity boundary conditions. At infinity of both universes we require $\psi_\ell\sim \mathrm{e}^{\pm \mathrm{i}\omega r_*}$, while at the throat the continuity of $\mathrm{d}\psi_\ell/\mathrm{d}r_*$ imposes either $\mathrm{d}\psi_\ell(r_0)/\mathrm{d}r_*=0$ or $\psi_\ell(r_0)=0$. Correspondingly, we find two families of QNMs for different values of the throat location r_0. Even in the black hole limit $r_0\to 2M$, the wormhole QNM spectrum is dramatically different from that of the Schwarzschild case. The QNMs of the wormhole approach the real axis and become long-lived.

This behaviour is related to the Z_2-symmetry of the effective potential V_ℓ: the potential has a second barrier for negative r_*, and as long as the throat is within the light ring, wormholes can support long-lived modes trapped between the two potential wells near the light rings.

2.2. Gravitational Waves Extraction

The energy flux emitted in gravitational waves is

$$\frac{\mathrm{d}E}{\mathrm{d}\omega}=\frac{1}{32\pi}\sum_{\ell\geqslant 2}\frac{(\ell+2)!}{(\ell-2)!}\,\omega^2\left|\psi_\ell(\omega,r\to\infty)\right|^2\,. \tag{3}$$

In the top panels of Fig. 1 we plot quadrupolar gravitational wave energy spectra for representative values of the throat position and the energy of the particle. We observe that they coincide only at low frequencies, but are generically very different.

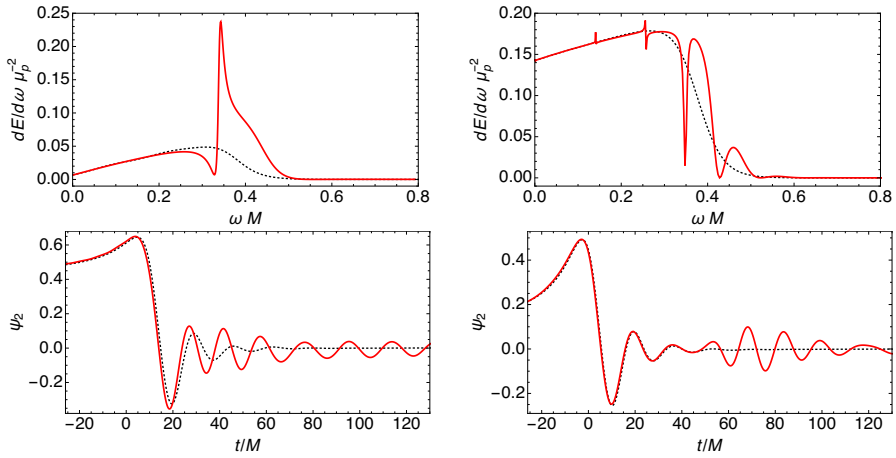

Figure 1. Top panels: $\ell=2$ gravitational wave energy spectra for a particle crossing a traversable wormhole (red solid line) compared to a particle plunging into a Schwarzschild black hole (black dotted line) with the same energy E. Bottom panels: The corresponding gravitational-wave waveforms. Left and right panels refer to $r_0=2.1M$, $E=1.1$ and $r_0=2.001M$, $E=1.01$, respectively.

Given the substantial differences in both the QNMs and energy spectra, we would expect a completely different ringdown signal. Nevertheless, in the bottom panels of Fig. 1 we observe that these differences do not leave any trace in the initial ringdown waveform. The actual QNMs of the wormhole get excited only at late times and contain low energy. As the wormhole approaches the black hole limit, $r_0 \to 2M$, the initial ringdown is precisely the same as in the Schwarzschild case.

3. Love Numbers

Tidal Love numbers describe the deformability of a self-gravitating object immersed in a tidal environment. A static, spherically symmetric compact object embedded in an external tidal field, characterised by a polar and axial tidal quadrupolar moment $\mathcal{E}$ and $\mathcal{B}$, develops in response a mass and current quadrupolar moment M_2 and S_2.[2] To the linear order, the induced quadrupole moments are proportional to the tidal moments, and the constants of proportionality are the polar and axial Love numbers,

$$k_2^E \equiv -\frac{1}{M^5}\sqrt{\frac{4\pi}{5}}\frac{M_2}{\mathcal{E}_{2\,0}}, \quad k_2^B \equiv -\frac{1}{M^5}\sqrt{\frac{4\pi}{5}}\frac{S_2}{\mathcal{B}_{2\,0}}\,, \tag{4}$$

where the numerical factor is conventional, M is the mass of the object and $\mathcal{E}_{2\,0}$ and $\mathcal{B}_{2\,0}$ are the $\ell = 2$, $m = 0$ components of the external tidal fields written in a basis of even- and odd-parity spherical harmonics $Y^{\ell\, m}$. The factor $1/M^5$, that makes the Love numbers dimensionless, is non-standard. It is much more common to divide by powers of the object radius, but since the definition of radius for boson stars can be equivocal, we adopt this non-standard choice.

To calculate the mass and current moments as functions of the external tidal field, we consider static $\ell = 2$ perturbations about a static spherically symmetric background spacetime, and adopt the Geroch-Hansen formalism [18, 19]. Such perturbations can be decomposed into even- and odd-parity sectors, and each sector must be a solution to the Einstein field equations linearised about the background metric. Finally, the quadrupolar moments, and consequently the Love numbers, can be extracted by matching the exterior solution to the asymptotic behaviour of the spacetime metric,

$$g_{tt} = -1 + \frac{2M}{r} + \sqrt{\frac{4\pi}{5}}\frac{2M_2}{r^3}\,Y^{2\,0} + \mathcal{O}\left(1/r^4\right) - r^2\,\mathcal{E}_2\,Y^{2\,0} + \mathcal{O}\left(r\right), \tag{5}$$

$$g_{t\varphi} = \frac{2J}{r}\sin^2\theta + \sqrt{\frac{4\pi}{5}}\frac{\sin\theta}{r^2}\,S_2\,\partial_\theta Y^{2\,0} + \mathcal{O}\left(1/r^3\right) + \frac{r^3\sin\theta}{3}\,\mathcal{B}_2\,\partial_\theta Y^{2\,0} + \mathcal{O}\left(r^2\right). \tag{6}$$

3.1. Love Numbers for Boson Stars and Gravastars

General relativistic boson stars have often been invoked as black hole mimickers, to explain dark matter halos and as generic dark matter candidates. They are self-gravitating solutions made entirely of fundamental, massive bosonic fields, described by the following action,

$$\mathcal{A} = \int \mathrm{d}^4x\,\sqrt{-g}\left(\frac{\mathcal{R}}{2\kappa} - |\partial\phi|^2 - V\left(|\phi|^2\right)\right). \tag{7}$$

Boson stars are usually classified according to their scalar potential, and their dynamics is described by the Einstein-Klein-Gordon equations. Assuming the spacetime to be spherically symmetric, the equilibrium configurations are obtained by numerically integrating the field equations supplied with regular boundary conditions at the origin and asymptotic flatness at infinity.

[2] It is relatively easy to generalise tidal fields and moments to higher-order multipoles, see [17].

Contrary to fluid stars, boson stars do not have a hard surface, as the scalar is spread out all over the radial direction. However, the configuration is highly localised in a radius $\sim 1/\mu$ and it is customary to define the effective radius R as the radius within which the 99% of the total mass M is contained. The compactness C of these objects, the ratio between mass and radius, can span from the same of planets to very close to that of black holes, *i.e.* 1/2.

Here we consider the simplest model: the free-field case, $V(|\phi|^2) = \mu^2|\phi|^2$, also known as minimal boson star, where μ is the mass of the bosonic field.

For the computation of the boson star Love numbers, we have considered only perturbations about stable equilibrium configurations. In the Regge-Wheeler gauge [20], the polar perturbations equations reduce to a system of two coupled equations, and to a single differential equation in the axial sector. We solve these equations supplemented by boundary conditions, we extract the mass and current moments by comparison with Eqs. (5) and (6), and then we compute the polar and axial Love numbers *à la* Hinderer [21],

$$k_2^E = \frac{8}{5}\Big((1-2\mathcal{C})^2[2\mathcal{C}(y-1)-y+2]\Big)\Big(3(1-2\mathcal{C})^2[2\mathcal{C}(y-1)-y+2]\ln(1-2\mathcal{C}) + 2\mathcal{C}\left[4\mathcal{C}^4(y+1)+2\mathcal{C}^3(3y-3)+2\mathcal{C}^2(13-11y)+3\mathcal{C}(5y-8)-3y+6\right]\Big)^{-1}, \tag{8}$$

$$k_2^B = \frac{8}{5}\frac{2\mathcal{C}(y-2)-y+3}{2\mathcal{C}\left[2\mathcal{C}^3(y+1)+2\mathcal{C}^2y+3\mathcal{C}(y-1)-3y+9\right]+3[2\mathcal{C}(y-2)-y+3]\ln(1-2\mathcal{C})}, \tag{9}$$

where $\mathcal{C} = M/r$ and $y \equiv rH'/H$ (being H the metric polar/axial perturbation function) evaluated at $r \gg R$. In the left panel of Fig. 2 we plot the polar and axial Love numbers for minimal boson stars and we observe that in the Newtonian regime, *i.e.* $M \to 0$, the polar Love number scales as $1/C^5$ while the axial scales as $1/C^4$.

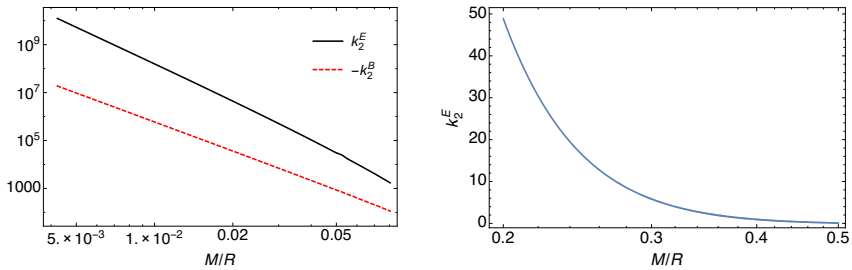

Figure 2. Quadrupolar $\ell = 2$ Love numbers for minimal boson stars (left) and thin-shell gravastars (right) as a function of their compactness.

A gravastar is another example of horizonless compact objects. Its interior is a de Sitter condensate, which is separated from the exterior Schwarzschild geometry by an intermediate region with finite thickness. In the thin-shell limit, the model is simple enough that the Love numbers can be computed analytically [22, 23].

In the right panel of Fig. 2, we see that polar Love numbers go to zero in the black hole limit and scale as $1/C^4$ for small compactness values.

3.2. Detectability

During the late inspiral phase, the tides between the binary affect the companions' gravitational field and orbital motion, and produce a measurable effect in the shape and the phasing of gravitational waves, accessible to measurements by Earth-based gravitational-wave detectors.

For neutron stars, tidal effects produce small corrections to the waveform phase which depends only on the star Love number [24].

Our results clearly show that Love numbers for boson stars and gravastar are in general not zero. When the detection of binary mergers will be ordinary, the gravitational-wave observations may be used to put upper bounds on the tidal Love numbers and constrain or rule out exotic alternatives.

4. Conclusions

To summarise, gravitational-wave astronomy has just begun and it provides a completely new instrument to explore the Universe.

In this work, we have seen that the initial ringdown signal chiefly depends on the properties of the light ring of the final object rather than its QNMs. The actual QNMs of the object are excited only at late times and typically do not contain a significant amount of energy. The events GW150914 and GW151226 strongly support the existence of light rings.

Future gravitational-wave detections should focus on extracting the late-time ringdown signal, where the actual QNMs of the final object are eventually excited and improve the signal-to-noise ratio. Such detections might eventually rule out exotic alternatives to black holes and test quantum effects at the horizon scale [25]. At the moment, the post-merger signal leaves room for alternative theories of gravity and exotic compact objects, such as gravastars and empty shells [26]. Furthermore, precise measurements of gravitational-wave signals in the earliest stages of the inspiral phase of the orbital evolution, and the subsequent extraction and comparison of the tidal Love numbers with the theoretical predictions can reveal important information about the internal structure of compact objects. This piece of information is — in principle — easy to extract as it is released cleanly well before the merger of the binary. It will shed light on the nature and the internal structure of black holes (allowing also for discrimination between general relativity and modified theories of gravity), and especially on the existence of exotic compact objects.

References

[1] Abbott B P *et al.* (LIGO/Virgo) 2016 *Phys. Rev. Lett.* **116** 061102
[2] Abbott B P *et al.* (LIGO/Virgo) 2016 *Phys. Rev. Lett.* **116** 241103
[3] Yunes N, Yagi K and Pretorius F 2016 *Phys. Rev.* **D94** 084002
[4] Abramowicz M A, Kluźniak W and Lasota J P 2002 *Astron. Astrophys.* **396** L31
[5] Liebling S L and Palenzuela C 2012 *Living Rev. Relat.* **15** 6
[6] Visser M 1996 *Lorentzian wormholes: From Einstein to Hawking* (Woodbury, USA: AIP)
[7] Mazur P O and Mottola E 2001 [gr-qc/0109035]
[8] Gimon E G and Hořava P 2009 *Phys. Lett.* **B672** 299
[9] Cardoso V, Crispino L C B, Macedo C F B, Okawa H and Pani P 2014 *Phys. Rev.* **D90** 044069
[10] Cardoso V, Franzin E and Pani P 2016 *Phys. Rev. Lett.* **116** 171101
[11] Steinhoff J, Hinderer T, Buonanno A and Taracchini A 2016 *Phys. Rev.* **D94** 104028
[12] Cardoso V, Franzin E, Pani P and Raposo G 2016 *In Press*
[13] Kokkotas K D and Schmidt B G 1999 *Living Rev. Relat.* **2** 2
[14] Berti E, Cardoso V and Starinets A O 2009 *Class. Quantum Grav.* **26** 163001
[15] Morris M S, Thorne K S and Yurtsever U 1988 *Phys. Rev. Lett.* **61** 1446
[16] Zerilli F J 1970 *Phys. Rev.* **D2** 2141
[17] Binnington T and Poisson E 2009 *Phys. Rev.* **D80** 084018
[18] Geroch R P 1970 *J. Math. Phys.* **11** 2580
[19] Hansen R O 1974 *J. Math. Phys.* **15** 46
[20] Regge T and Wheeler J A 1957 *Phys. Rev.* **108** 1063
[21] Hinderer T 2008 *Astrophys. J.* **677** 1216
[22] Pani P 2015 *Phys. Rev.* **D92** 124030
[23] Uchikata N, Yoshida S and Pani P 2016 *Phys. Rev.* **D94** 064015
[24] Flanagan É É and Hinderer T 2008 *Phys. Rev.* **D77** 021502
[25] Giddings S B 2016 *Class. Quantum Grav.* **33** 235010
[26] Cardoso V, Hopper S, Macedo C F B, Palenzuela C and Pani P 2016 *Phys. Rev.* **D94** 084031